THE ORIGIN OF HIGH ENERGY COSMIC RAYS DISPLAYED BY THE ENERGY SPECTRUM AND ELEMENTAL COMPOSITION*

H. Rebel

for the KASCADE Collaboration

Forschungszentrum Karlsruhe, Institut für Kernphysik
76021 Karlsruhe, Germany

(Received December 28, 1999)

In spite of lapse of time of nearly 90 years since the discovery of cosmic rays, the basic questions: "Where are cosmic rays coming from? How are they accelerated to extremely high energies and propagate through the interstellar and intergalactic space?" are largely not clarified. Contemporary theoretical models describe the acceleration of nuclei in the Cosmos by strong shocks, either of galactic or extragalactic origin, which are effectively produced in supernova remnants, supersonic stellar winds, active galactic nuclei and other phenomena. All the models and conjectures towards an explanation of the energy spectrum, in particular of the conspicuous discontinuity ("knee") observed in the energy region of about $3\cdot 10^{15}$ eV, do not only predict the shape of the spectrum, they imply also specific variations of the elemental composition of the primary cosmic rays. The lecture discusses the experimental approaches investigating the shape of the primary spectrum and the elemental composition of cosmic rays.

PACS numbers: 94.40.Lx, 94.40.Pa

1. Introduction

A most conspicuous feature of the energy spectrum of primary cosmic rays is a distinct change of the spectral index of the power-law fall off around 10^{15} eV, called the "knee". This feature has been discovered exactly 40 years ago by German Kulikov and George Khristiansen from the Moscow State University with studies of the intensity spectrum of Extensive Air Showers (EAS) [1]. Since that time the problem of the astrophysical origin of this

* Invited talk presented at the XXVI Mazurian Lakes School of Physics, Krzyże, Poland, September 1–11, 1999.

phenomenon is with us. All models and conjectures towards an explanation do not only predict the *shape of the spectrum* and the position of the knee *e.g.*, they imply also specific *variations of the elemental composition* of the primary cosmic rays. A recent hypothesis of a single near positioned supernova [2], whose production spectra are considered to be superimposed to the overall galactic contribution leeds to conspicuous modulations of the energy spectrum around the knee, attributed to composition changes. Thus the mass or elemental composition of high energy cosmic rays is an issue of utmost importance and actual interest. The investigation of the detailed spectral shape and, in particular, of a conjectured variation of the mass composition of the knee region, are the objectives of a number of contemporary large scale experiments like the KASCADE experiment [3], set up in Karlsruhe (Germany) to which this contribution mostly refers.

In the region above 10^{14} eV the only access to the properties of the primary radiation is the observation of air showers induced in the Earth's atmosphere by the primary cosmic particles. The present report emphasizes the methodical concepts rather than actual results of current experiments which still display an inconsistent picture.

2. Extensive Air Showers (EAS)

The measurements of cosmic rays at ground level present an obvious and tremendous problem: the primary particles interact within the atmosphere and what is observed on ground is very different from what arrives from the space. EAS experiments are the attempt to infer the properties of the primaries after an absorber of about 1 kg/cm^2. A primary proton *e.g.* interacts about a dozen times with the air atoms before reaching the ground. In each collision a considerable number of particles is produced, most with sufficient energy to generate more particles in further interactions. Most of the produced particles in the hadronic interactions are pions and kaons, which can decay into muons and neutrinos before interacting, thus producing the most penetrating component of atmospheric showers. The most intensive component — electrons and photons — originates from the fast decay of neutral pions into photons, which initiate electromagnetic showers, thus distributing the originally high energy of the primary over millions of charged particles. The backbone of an air shower is the hadronic component of nucleons, pions and more exotic particles.

In ground-based experiments, from the EAS parameters observed in a certain stage of development, *i.e.* from the intensity, the lateral and eventually the energy distributions of the main EAS components, we have to deduce the properties of the primary particle. In a typical EAS experiment the lateral distributions of the particles are sampled by more or less regular arrangements of a large number of particle detectors which cover only a small fraction of the total area. This sampling may be an additional source of fluctuations which add to the large spread resulting from the inherent statistical fluctuations of the shower development in the atmosphere.

3. Principles of EAS inference

The general scheme of inference in a modern EAS experiment is displayed in Fig. 1, indicating also the involved difficulties.

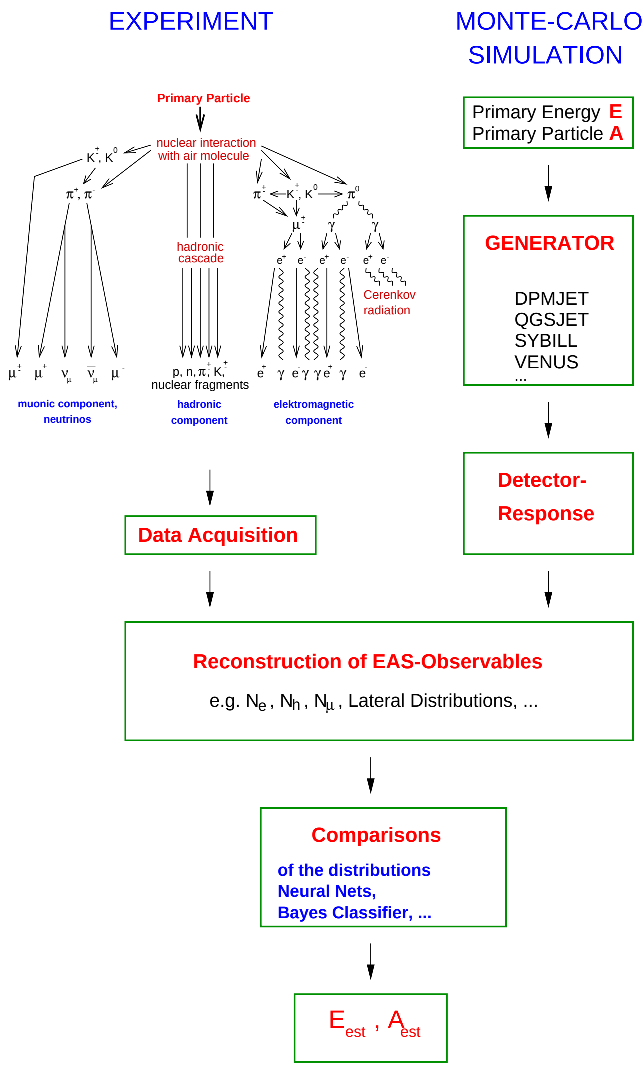

Fig. 1. General scheme of the analysis of EAS observations.

The identification of differences in EAS which result from differences in mass of the primary particle requires a modeling of shower development in the atmosphere. For that Monte Carlo programs of the EAS development like the Karlsruhe CORSIKA program [4] have been developed. It is under continuous modification and improvement. A prerequisite for the Monte Carlo procedures is a knowledge about particle production in high-energy hadronic interactions. Since the energy region of our interest exceeds the particle energies provided at man made accelerators, we rely on model descriptions which extend the present knowledge to a terra incognita, on basis of more or less detailed theoretical approaches of phenomenological nature and with QCD inspired ideas. The CORSIKA code includes various models (see Ref. [5]), presently en vogue as options, and in fact, the model dependence is an obvious feature in the actual comparisons with the experimental data.

On the other side a multi-detector experiment observing simultaneously all major EAS components with many observables provides some possibilities to test the hadronic interaction models and to specify the most consistent one.

The stochastic character of the huge number of cascading interactions in the shower development implies considerable *fluctuations* of the experimentally observed EAS parameters and of the corresponding simulated showers as well, clouding the properties of the original particle. The inherent (unavoidable) fluctuations establish an important and intriguing difficulty of the EAS analysis and need adequate response of the analysis methods.

The further processing is to compare real data with pseudo experimental data on equal level, including the detector response and expressed by various reconstructed shower variables: *intensity, the lateral distributions, arrival time and eventually energy distributions of the various EAS components.* With this comparison step we have to realize: None of the observables is strictly only dependent on the mass of primary, or only dependent from the energy, and since we are investigating an *a priori* unknown spectral distribution accompanied by an *a priori* unknown variation of the elemental composition (or vice versa), there is always an intriguing feedback of the estimates of both. Therefore multivariate analyses, correlating the observations of different EAS variables are strongly required, and the inference from only one EAS component has been often misleading.

The comparisons can be made in a first step by use of *averaged quantities* introducing *plausible parameterizations* of the simulation results, or alternatively on event-by-event basis by *multivariate nonparametric analyses invoking advanced statistical decision methods* [6]. Only in the latter case we do adequately take into account the shower fluctuations and are able to specify in a transparent way, how conclusive our results really are, by quoting Bayes errors and through true- and mis-classification matrices of the results.

4. EAS signatures of the primary mass

In simulation calculations we notice a different development of heavy ion induced air showers due to the smaller interaction length and due to the larger number of nucleons in the projectile, combined with the effect that the multiplicity of secondary particle production per nucleon varies only slowly with the energy. Thus the muon content of an iron induced EAS *e.g.* appears to be larger than for the proton induced one. Simultaneously the number of electromagnetic particles (electrons) is larger in the proton EAS, because their energies reflect the energies of the neutral pions from which they originate. As the electrons and positrons are rapidly absorbed when their energies drop below ca. 100 MeV, an A-nucleon shower (with each primary nucleon carrying the energy E/A) reaches earlier the maximum, *i.e.* higher in the atmospheric altitude. That means that for the same primary energy E the shower sizes N_e are different for different kind of primaries registrated at observation level.

4.1. N_e–N_μ correlation

Monte Carlo simulations reveal the mass-sensitive correlation of the muon number with the electron number. Actually the N_e–N_μ correlation is the most powerful discriminator, and all other signatures just help to shrink the fluctuations and the model dependence, especially the hadronic observables do so. The predicted correlation is dependent from the particular interaction model (see Ref. [5]). Unfortunately the experimental application of the N_e–N_μ correlation implies some practical difficulties. In most detector arrays, if the muon detectors are not extremely shielded, the punch-through of the electromagnetic component in the shower center spoils the discrimination of muons there. In addition, due to the large lateral extension and fluctuations of the muon component at large distances from the shower center the extrapolations of the lateral distribution appear rather uncertain. As a consequence, the total number N_μ is rather difficult to determine in a way, unbiased by assumptions.

From these reasons the KASCADE experiment applies the correlation method in a modified variant, using as observable the socalled truncated muon number N_μ^{tr}, the integrated muon intensity between 40 and 200 m from the shower core. Shown by simulations, as consequence of a fortunate interference of effects arising from different shapes, energy distributions and intensities for the KASCADE conditions, this quantity proves to be nearly independent from the mass of the primary and is proportional to primary energy in range of 10^{14} to 10^{16} eV. That is at expense of the mass discrimination, which now is only due to the different development of the electromagnetic component at the same energy.

In a recent parametric analysis of KASCADE data (based on 140 million events) [7], the data have been divided in different energy bins. The $\log N_\mu^{\rm tr} / \log N_e$ parameter (shown in Fig. 2 for $\log E\,(\mathrm{GeV}) = 6.1$–$6.3$) has been approximated by a Gaussian shape. The mean values and spread of the distributions of four mass groups have been parameterized as functions of the reconstructed energy. The sum of these functions has been fitted for each energy bin to the data resulting in fractions of the considered mass groups (P, He, O, Fe).

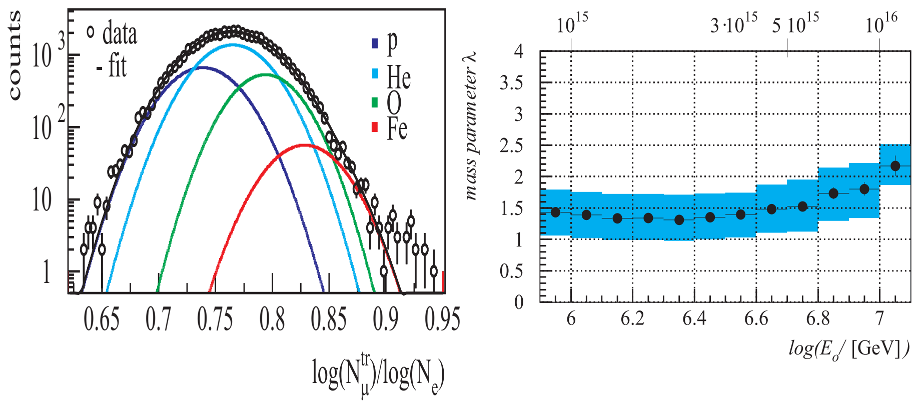

Fig. 2. Parameterization of the $\log N_\mu^{\rm tr} / \log N_e$ ratio and the energy dependence of the mean logarithmic mass [7].

With this parametric procedure the variation of the mass composition is inferred. Below the energy of $\log E\,(\mathrm{GeV}) = 6.5$–$6.6$, there is little change of a light mass dominated composition. After the knee position there appears a decrease in the light elements and an increase of the heavy contributions. This is displayed by a mass parameter $\lambda = \sum_i \ln(A_i) \cdot P_i$ (summed over all mass components), increasing here from 1.4 ± 0.3 below the knee to 2.1 ± 0.3 at 10^{16} eV. The error stems only from the restricted statistical accuracy of the limited number of simulated showers.

4.2. Structure of the shower core

Further signatures of the mass composition are due to effects which arise from the transverse momentum distributions of the secondaries. The smaller deflection angles in proton induced showers lead to a steeper lateral distribution. This is particularly pronounced for the penetrating muon component, which is less absorbed and less deflected by Coulomb scattering and carries original information about the air shower cascade. Consequences of these features of the lateral distributions together with the differences in the energy spectra are observable differences, in particular, in the appearance of the muonic and hadronic components in shower center of EAS of different mass primaries.

Experimental studies have been performed in the KASCADE experiment [8] with the central detector. The characteristica of the patterns of the particle distributions can be quantified by a parameterization in terms of multifractal moments, which have been shown by the simulation studies to be significant in view of mass information.

4.3. Observations informing about the longitudinal development

The shape of the lateral distributions of each EAS component, especially however of penetrating, less absorbed particles carry some information about the stage of the shower development. For the charged particles components this is traditionally expressed by the age-parameter, which enters in the lateral distribution function and indicates the stage of EAS development.

High-energy charged particles generate Cerenkov radiation which is strongly forward peaked and can be detected on ground. It is emitted by the shower cascade throughout the atmosphere and offers the possibility of measuring the total energy of the shower and of tracing the rate of building up the shower. Due to the changing refractive index and the characteristic Cerenkov angle the lateral distribution has a particular structure, and the shape of the distribution around 100 m gets sensitive to the height of emission. The light from the early part, where the energy of the particles are still very high and the scattering angles small is concentrated in a characteristic ring near 100 m. The resulting lateral distribution is the superposition from all heights and its shape depends on the shower development. If the shower maximum gets nearer to the ground, more light is produced near the shower core. That means the lateral distribution drops steeper the closer the shower maximum approaches the detector. There is a correlation between the the distance to the shower maximum and a slope parameter of the Cerenkov light distribution $\rho_c = \rho_0 \cdot \exp(R \cdot \mathrm{slope})$. The correlation proves to be independent of the type of the particle and the angle-of-shower incidence.

In the HEGRA AIROBIC experiment [9] in La Palma, Spain (2200m a.s.l.), equipped with a scintillator array measuring the charged particle component (N_e, angle of shower incidence and core position) and with an array of open photomultipliers for the Cerenkov light registration, the Cerenkov light is analysed only in the interval 20-100 m from the shower core.

In observations of the Cerenkov light by the imaging technique like in the experiment DICE (Dugway) [10] cosmic ray events within the field of view produce a focal plane image at the photomultiplier that is the intensity pattern of Cerenkov light coming from the air shower. When the direction of the air shower and the distance of the shower core from the telescopes *are known, simple geometry can be used to reconstruct the amount of light received from each altitude of the shower, as the amount of light is strongly correlated with the shower size as function of the depth in the atmosphere from which the height of maximum $X_{\max}$ can be determined. This procedure is essentially geometrical and is so far independent from Monte Carlo simulations. However, the interpretation of the observed $X_{\max}$ distribution, which plays now the role of a shower parameter, in terms of the elemental composition will again need the Monte Carlo simulations with all the inherent model dependence.*

What is the information about the mass of the primary when having determined the depth of the shower maximum?

The change of the position of the depth of the EAS maximum with the energy per decade, the socalled elongation rate, is fairly constant. As consequence of the superposition model approximation *i.e.* assuming that for the heavy primary (A) the $X_{\max}$ dependence scales with E/A, the mean atmospheric depth of the maximum depends only from the energy per nucleon of the primary. This is confirmed by simulations, but showing also considerable fluctuations, decreasing with the nucleon number A. With the mean E/A deduced from $X_{\max}$ of maximum we gain information about the average mass, if independently the energy E of the primary can be determined [11]. Thus finally the $X_{\max}$-dependence from the energy E is compared with simulation predictions (see Fig. 3).

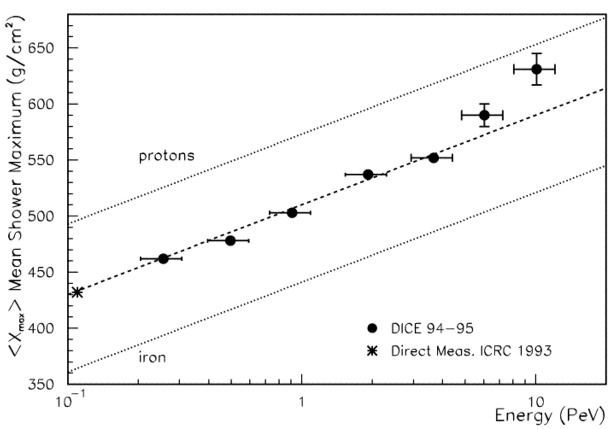

Fig. 3. The variation of the atmospheric depth $X_{\max}$ of the EAS maximum from Cerenkov light observations of the DICE experiment [10].

The variation of the mass composition around the knee deduced from the DICE (Dual Imaging Cerenkov Experiment) [10] observations (Fig. 3) is contradictory to the preliminary KASCADE and many other results. It should be noted, so elegant the Cerenkov experiments may appear, they infer the elemental composition from only few observational parameters, and that essentially of one single EAS component.

A very interesting alternative way of looking for information on the longitudinal development are measurements of muon arrival time and their angle-of-incidence distributions at muon energies, when absorption and Coulomb scattering have become negligible. As compared to the principal possibility to analyse also arrival time distributions of Cerenkov photons, which are in a highly nonlinear relation to production heights [12], in the case of muons the mapping appears to be rather simple and approximately geometrical [13].

Actually measurements of muon arrival time distributions for muon energies $> 2\,\mathrm{GeV}$ have been performed in KASCADE [14], and analyses in view of their information about mass composition are in progress.

5. Multivariate approach

The concept of the KASCADE experiment with a multi-component detector array is to measure a larger number of EAS variables for each individual event with high accuracy. For this aim the detector has been specially designed. Specific EAS variables accessible in addition to the shower size N_e and the truncated muon number N_μ^{tr} are the number of hadrons N_h^{100} with energies larger than 100 GeV, the energy sum $\sum E_h$ of these hadrons, the energy of the most energetic hadron $E_h^{\max}$ in the shower, the number $N_\mu^\star$ of muons with energies larger than 2 GeV and others like some quantities representing the muon arrival time distribution.

For the analysis of the correlated distribution without any bias of a parameterization, there are adequate methods worked out involving neural networks and Bayesian decision making. We shall not discuss these techniques, but let me mention that for each particular case *i.e.* for a particular set of selected EAS variables or for a chosen number of mass groups or for a specific hadronic interaction model generating the pattern to be compared, matrices for true- and misclassification are obtained. From that measures for the confidence and errors can be constructed.

The diagrams (Fig. 4) display examples of the reconstructed chemical composition and the mean mass *vs.* energy identifier N_μ^{tr} (the knee is at $\log N_\mu^{\mathrm{tr}} = 4.1$) taking four EAS observables into account. Compared are the results obtained with two different hadronic interaction models QGSJet and VENUS and the cases with two and three mass groups. We recognize again the tendency that the lighter composition before the knee gets heavier beyond. The QGSJet model leads generally to a heavier composition. The reconstructed mean mass depends obviously also from the number of mass classes.

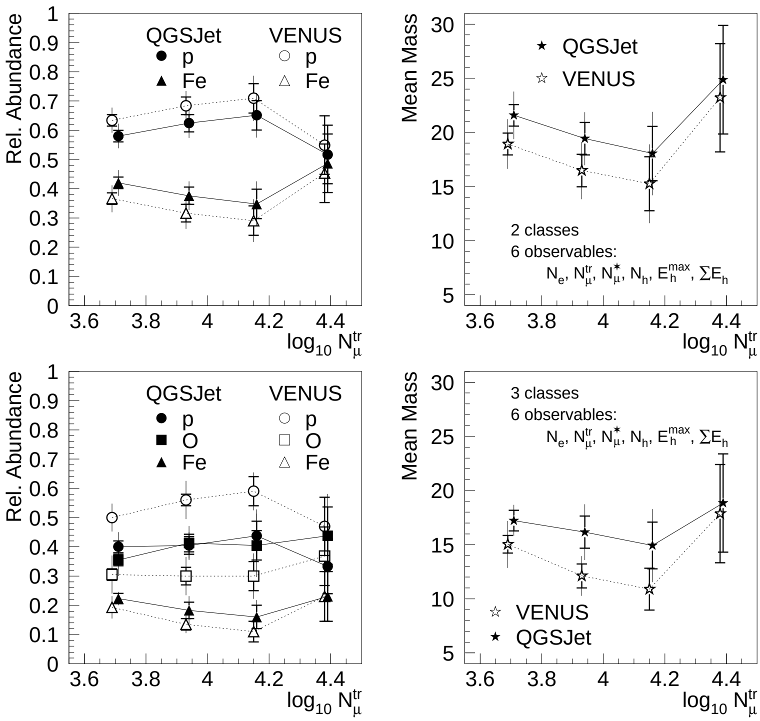

Fig. 4. Reconstructed variation of the composition and mean mass [15].

This is a result of a feasibility study [15], and actually it suffers from the limited statistical accuracy, especially due to the limited number EAS with the hadronic core observed. But it points to the way, how the data can be consistently analysed on event-by-event basis with an exploration of the particular sensitivities and quantitative specification of the uncertainties, arising from the model dependence *e.g.*

6. Spectra and composition

Finally the interrelation of the determination of the primary energy spectrum and of the varying mass composition is sketched. In the KASCADE experiment the knee has been observed in all EAS components, most accurately in the shower size N_e and in the muon content N_μ spectra. The task is to translate the observed spectra of the EAS variables into the primary energy spectrum in a consistent way, determining the position of the knee and the spectral indices before and beyond. This can be achieved via EAS simulations and with adjusting the variation of the mass composition [16].

EAS simulations provide the bridge for mapping $logE \rightarrow logN_{e,\mu}$, finally seriously taking into account the detector response and the fluctuations for each type of considered primaries by integral equations of Fredholm type with the kernels $p_A(logE \rightarrow logN_{e,\mu})$, derived from EAS simulations (A: H,.....Fe):

$$\frac{dJ_A}{d\,\log N_{e,\mu}} = \int \frac{dJ_A}{d\,\log E}\, p_A(\log E \rightarrow \log N_{e,\mu})d\,\log E\,.$$

Fig. 5 shows the result of such a procedure obtained on basis of an *a priori* adopted power-law spectral form.

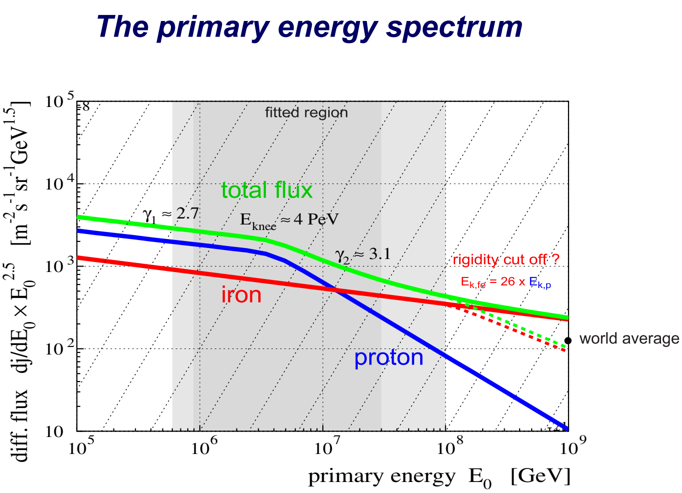

Fig. 5. Analysis of the N_e and N_μ spectra in view of the mass composition [16].

7. Concluding remarks

This talk tried to focus your attention to various EAS signatures of the primary mass and procedures of analyses of air shower observations in terms of the energy variation of the mass composition, especially for the knee region. The illustration has been strongly weighted with recent results of the KASCADE experiment. In fact it is the only approach which observes — shower per shower — all three main components by various different observables. This seems to be indispensable on the way to remove and to clarify the observed inconsistencies, which are supposed — and we have arguments for that — to arise mainly from an insufficient description of the high-energy hadronic interaction by the current models [17].

This is based on recent results of the KASCADE experiment. In particular, I acknowledge the valuable discussions with Dr. A. Haungs and Dr. M. Roth.

REFERENCES

[1] G.V. Kulikov, G.B. Khristiansen, *Sov. Phys. JETP* **358**, 441 (1959).

[2] A.D. Erlykin, A.W. Wolfendale, *Astrophys. J.* **7**, 1 (1997).

[3] K.-H. Kampert *et al.*, KASCADE collaboration, Proc. 16th European Cosmic Ray Symposium, Alcala, Spain: Rayos Cosmicos, 1998 p.547, eds. J.Medina *et al.*, Universidad de Alcala, Spain.

[4] D. Heck, J. Knapp, J.N. Capdevielle, G. Schatz, T. Thouw, Report FZKA 6019 (1998), Forschungszentrum Karlsruhe.

[5] J. Knapp, D. Heck, G. Schatz, Report FZKA 5828 (1996), Forschungszentrum Karlsruhe; J. Knapp, Rapporteur talk, 25th ICRC 1997, Durban, Vol.8, 83.

[6] A.A. Chilingarian *et al.*, *Nucl. Phys. B (Proc. Suppl.)* **52B**, 237 (1997); *Nucl. Phys. B (Proc. Suppl.)* **52B**, 240 (1997).

[7] J.H. Weber *et al.*, KASCADE collaboration, Proc. 26th ICRC, 1999, Salt Lake City, Utah, HE 2.2.42.

[8] A. Haungs *et al.*, KASCADE collaboration, Proc. 26th ICRC, 1999, Salt Lake City, Utah, HE 2.2.39; A. Haungs *et al.*, *Nucl. Instrum. Methods* **A372**, 515 (1996).

[9] A. Lindner *et al.*, HEGRA collaboration, Proc. 25th ICRC, 1997, Durban, Vol. 5, p.113; A. Lindner, *Astrophys. J.* **8**, 235 (1998).

[10] K. Boothby *et al.*, *Astrophys. J.* **491**, L35 (1997).

[11] J. Cortina, F. Arqueros, E. Lorenz, *J. Phys. G: Nucl. Part. Phys.* **23**, 1733 (1997).

[12] A.M. Hillas, *J. Phys. G: Nucl. Phys.* **8**, 1475 (1998).

[13] H. Rebel *et al.*, *J. Phys. G: Nucl. Part. Phys.* **21**, 451 (1995); H. Rebel, Proceedings XV Cracow Summer School of Cosmology, The Cosmic Ray Mass Composition, Lodz, Poland, 15–19 July, 1996, ed. W. Tkaczyk, p. 91.

[14] I.M. Brancus *et al.*, KASCADE collaboration, Report FZKA 6151(1998), Forschungszentrum Karlsruhe; T. Antoni *et al.*, KASCADE collaboration, *Astrophys. J.*, to be published.

[15] M. Roth, Report FZKA 6262 (1999), Forschungszentrum Karlsruhe; M. Roth *et al.*, KASCADE collaboration, Proc. 26th ICRC, 1999, Salt Lake City, Utah, HE 2.2.40.

[16] R. Glasstetter *et al.*, KASCADE collaboration, Proceedings 26th ICRC, 1999, Salt Lake City, Utah, HE 2.2.03.

[17] H. Rebel, KASCADE collaboration, Proc. Int. Symposium Nuclear Electro-Weak Spectroscopy, NEWS 99, Osaka, Japan, March, 9–12, 1999; T. Antoni *et al.*, KASCADE collaboration, *J. Phys. G: Nucl. Part. Phys.*, in press.